

# Supporting Information

## Significant underestimate of gaseous Methanesulfonic Acid (MSA) over Southern Ocean

Jinpei Yan<sup>\*1,2</sup>, Jinyoung Jung<sup>3</sup>, Miming Zhang<sup>1,2</sup>, Suqing Xu<sup>1,2</sup>, Qi Lin<sup>1,2</sup>, Shuhui Zhao<sup>1,2</sup>, Liqi  
Chen<sup>\*1,2</sup>

*1 Key Laboratory of Global Change and Marine-Atmospheric Chemistry, MNR, Xiamen 361005, China;*

*2 Third Institute of Oceanography, Ministry of Natural Resources, Xiamen 361005, China;*

*3 Korea Polar Research Institute, 26 Songdomirae-ro, Yeonsu-gu, Incheon 21990, Republic of Korea*

Corresponding author: Jinpei Yan, E-mail address: [jpyan@tio.org.cn](mailto:jpyan@tio.org.cn)

The supplementary information contains 10 pages, including 1 table and 7 figures. The table and figure captions are listed as follow:

Tab. S1 Gaseous and particulate MSA levels in different regions;

Fig. S1 Gases and aerosols monitoring system using in this study;

Fig. S2 Calibration curves of MSA, chloride, sulfate and sodium for IGAC monitoring system;

Fig. S3 Time series of particulate sodium and sulfate during the observation cruise;

Fig. S4 Time series of  $MSA_g$ ,  $MSA_p$ ,  $nss-SO_4^{2-}$ , and the meteorological parameters during  
November 2017 to February 2018;

Fig. S5 Spatial distributions of sea ices and Chlorophyll-a concentrations;

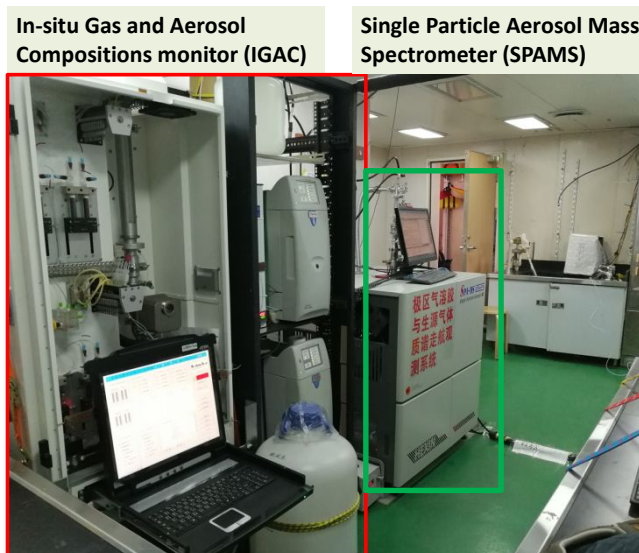
Fig. S6 Time series of the ratios of  $MSA_g$  to  $MSA_p$  during the whole cruise;

Fig. S7 Correlation between  $MSA_g$  to  $nss-SO_4^{2-}$  ratios and  $MSA_T$  to  $nss-SO_4^{2-}$  ratios.

Tab. S1 Gaseous and particulate MSA levels in different regions

Region	Longitude	Latitude	MSA <sub>g(min)</sub>	MSA <sub>g(max)</sub>	MSA <sub>g(Avg.)</sub>	MSA <sub>p(min)</sub>	MSA <sub>p(max)</sub>	MSA <sub>p(Avg.)</sub>
	(°E)	(°S)	(pptv)	(pptv)	(pptv)	(ng•m <sup>-3</sup> )	(ng•m <sup>-3</sup> )	(ng•m <sup>-3</sup> )
Leg I	76 - 177	43 - 75	-	24.5	5.9±4.7	14.6	392.6	45.5±32.0
Leg II	72 - 185	43 - 78	-	13.0	2.4±0.7	0.3	165.4	33.7±24.8
MA1	173	43 - 51	12.7	24.4	19.5±5.2	73.2	167.0	99.6±22.9
MA2	172	64 - 69	3.9	24.5	11.7±5.1	49.5	392.6	84.0±38.3
MA3	125 - 142	63	3.5	5.0	4.2±0.5	50.8	95.0	61.7±16.3
MA4	85 - 93	61.5	2.6	3.3	2.9±0.2	43.3	144.9	57.4±24.6
MA5	170 - 185	68.2 - 77.8	1.4	4.0	2.4±0.6	57.4	165.4	100.3±18.6
MG1	163 - 177	72 - 75	5.0	21.4	6.7±2.2	20.8	75.0	38.4±21.9
MG2	101 - 106	62	4.8	5.7	5.3±0.3	36.7	71.8	45.5±9.6

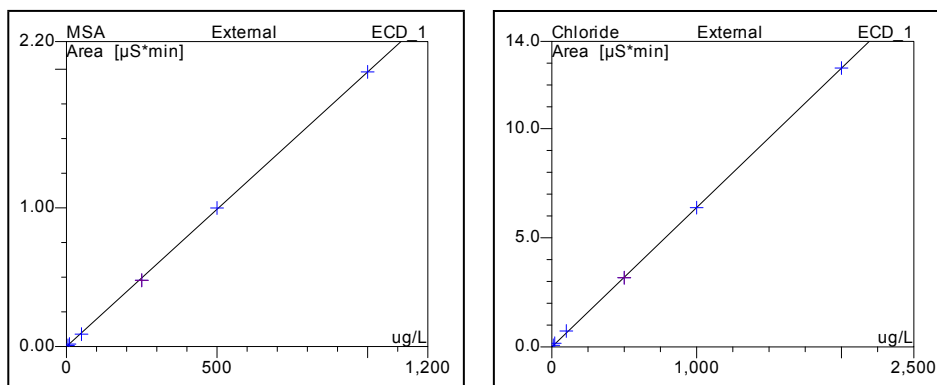
27 Fig. S1 Gases and aerosols monitoring system. An underway biogenic gases and aerosols  
28 monitoring system were employed on the R/V “Xuelong” to carried out the observation in the SO.  
29 An In-situ Gas and Aerosol Composition monitoring system was used to determine the gaseous  
30 and aerosol water-soluble ions. A Single Particle Aerosol Mass Spectrometer was used to  
31 determine the particle size distribution and chemical compositions.



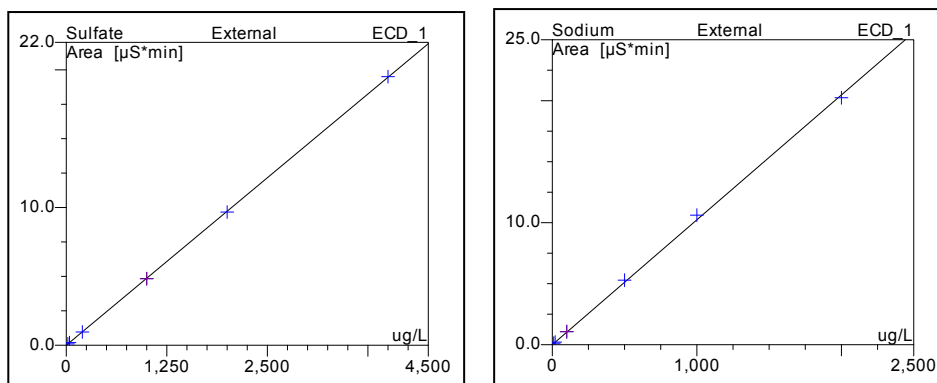
32  
33

34 Fig.S2 Calibration curves of MSA, chloride, sulfate and sodium for IGAC monitoring system. (a)  
35 Six out of eight concentrations of standard solutions (0.1-1000 ug/L) were selected for MSA  
36 calibration ( $r^2=0.998$ ); (b) Six out of eight concentrations of standard solutions (0.1-2000 ug/L)  
37 were selected for Chloride calibration ( $r^2=0.997$ ); (c) Six out of eight concentrations of standard  
38 solutions (0.1-4000 ug/L) were selected for Sulfate calibration ( $r^2=0.997$ ); (d) Six out of eight  
39 concentrations of standard solutions (0.1-2000 ug/L) were selected for Sodium calibration  
40 ( $r^2=0.998$ ).

41

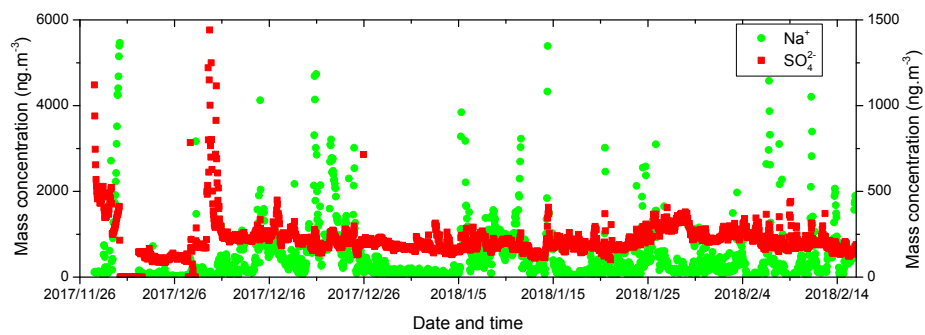


42



43

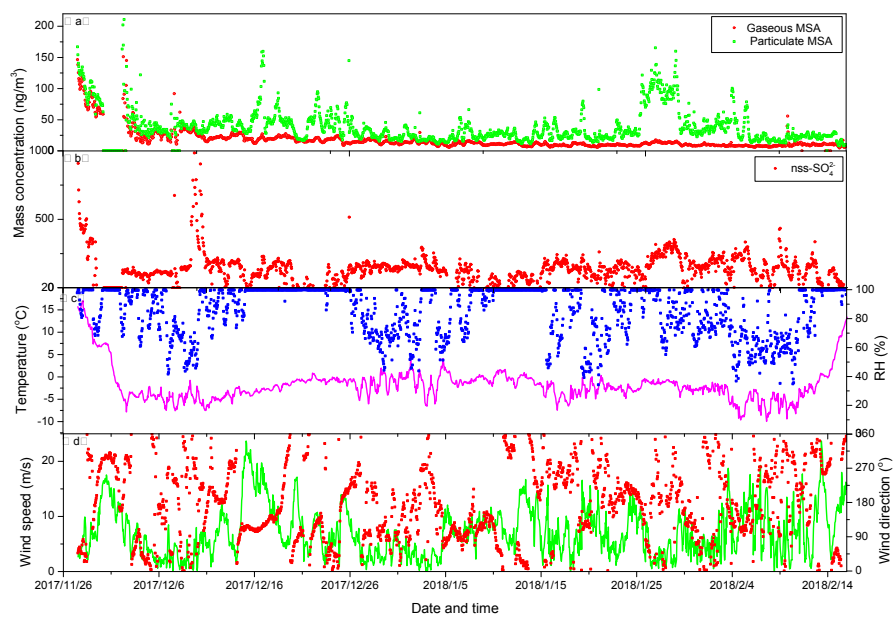
44 Fig. S3 Time series of particulate sodium and sulfate during the observation cruise.



45

46

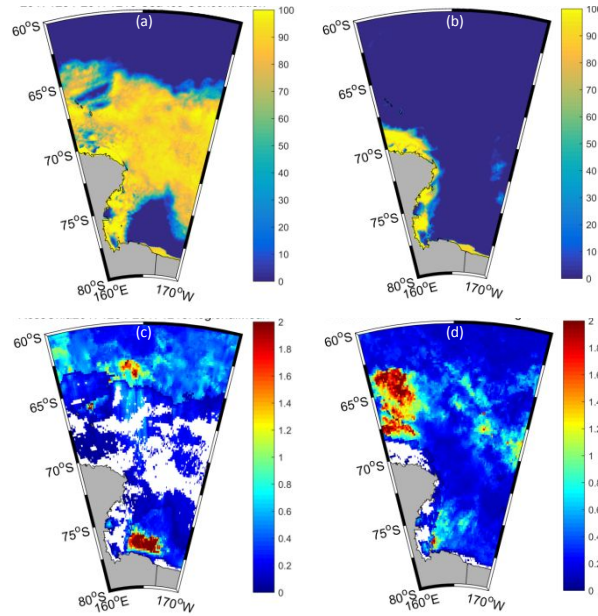
47 Fig. S4 Time series of gaseous and particulate MSA, nss-SO<sub>4</sub><sup>2-</sup>, and meteorological parameters  
48 during Nov. 2017 to Feb. 2018. (a) Temporal distributions of gaseous and particulate MSA; (b)  
49 Temporal distribution of nss-SO<sub>4</sub><sup>2-</sup>; (c) Temperature and RH; (d) Wind speed and directions.



50

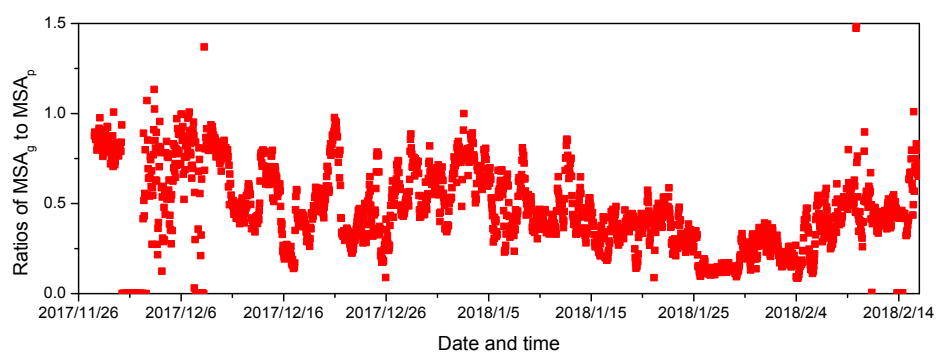
51

52 Fig. S5 Spatial distributions of sea ice and Chl-a concentrations. (a) Average sea ice during 4 to 14  
53 December, 2017; (b) Average sea ice during 25 January to 4 February, 2018; (c) Mean Chl-a  
54 concentrations during 4 to 14 December, 2017; (d) Mean Chl-a concentrations during 25 January  
55 to 4 February, 2018. The Spatial distributions of sea ice and Chl-a concentrations in this figure  
56 were created with Ocean Data View (Ref.S1 and S2).



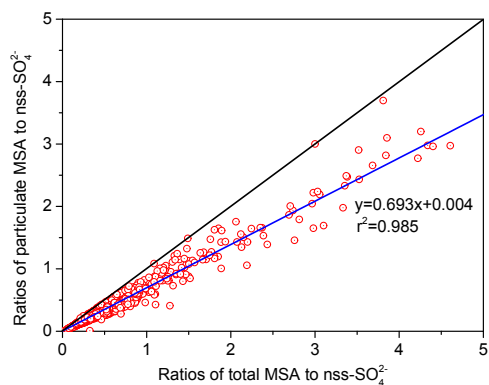
57  
58

59 Fig. S6 Time series of the ratios of  $MSA_g$  to  $MSA_p$  during the whole cruise.



60

- 61 Fig. S7 Correlation between  $\text{MSA}_g$  to  $\text{nss-SO}_4^{2-}$  ratios and total  $\text{MSA}_T$  to  $\text{nss-SO}_4^{2-}$  ratios. An  
62 intensity positive correlation between  $R_p$  and  $R_T$  ( $r^2= 0.985$ ) was observed, with a slope of 0.693.  
63 The ratios of  $\text{MSA}$  to  $\text{nss-SO}_4^{2-}$  were reduced by about 30 % without  $\text{MSA}_g$ .



64

66 **References**

67 S1. Schlitzer, R. Ocean Data View, odv.awi.de, 2015.

68 S2. Schlitzer, R. Interactive analysis and visualization of geosciences data with Ocean Data view. *Computers*  
69 *Geosciences*. 2002, 28, 1211-1218.

70